Electronic Supplementary Material (ESI) for Soft Matter.
This journal is © The Royal Society of Chemistry 2014

Hollow magnetic microspheres obtained by nanoparticle adsorption on surfactant stabilized microbubbles

Artem Kovalenko[1,2], Julien Jouhannaud[2], Prasad Polavarapu[1], Marie Pierre Krafft[1], Gilles Waton[1], Geneviève Pourroy[2*]

[1] Institut Charles Sadron (ICS) CNRS - Université de Strasbourg (UPR 22). 23 rue du Loess, BP 84047. 67034 Strasbourg Cedex 2. France

[2] Institut de Physique et Chimie des Matériaux de Strasbourg IPCMS, UMR 7504 CNRS-ECPM-Université de Strasbourg, 23 rue du Loess BP 43, 67034 Strasbourg cedex 2 France

*** corresponding author: genevieve.pourroy@ipcms.unistra.fr**

Supplementary information

1) Magnetization curve of $CoFe_2O_4$ nanoparticles

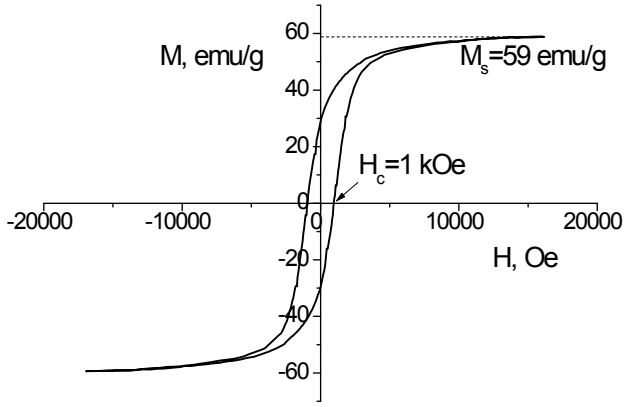

Figure SI-1 – Magnetization curve of $CoFe_2O_4$ NPs.

2) pH effect on the stabilization of microbubbles by the *F*8*H*2Phos surfactant.

Figure SI–2 shows a photograph of vials containing solutions of 1.25 mM *F*8*H*2Phos and 0.1 M NaCl at five different values of pH after manual shaking for 10 seconds. The solutions at pH 5.6 – 8.5 are turbid due to the microbubble formation. The number of bubbles increases when the pH increases from 5.6 up to 8.5. The microbubbles disappear for higher pH. In this work we choose the pH 8.5 to stabilize the microbubbles with NPs.

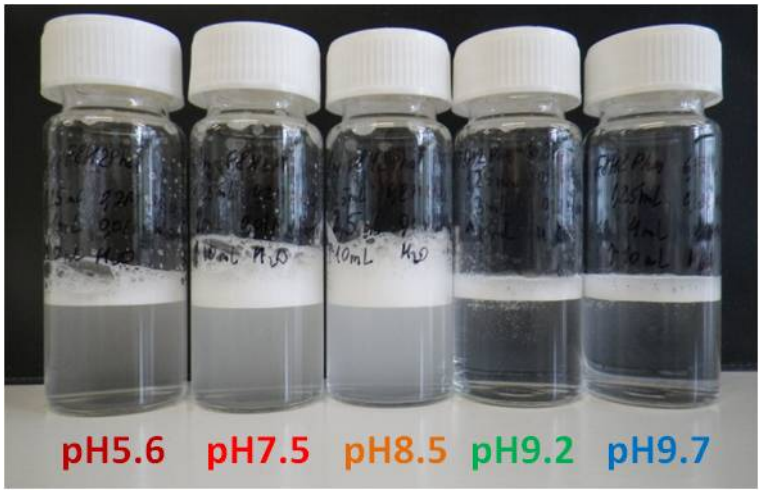

Figure SI-2- Images of *F*8*H*2Phos surfactant solutions after stirring at various pH.

3) Morphology of *F*8*H*2Phos-stabilized microbubbles.

Figure SI-3 shows two optical microscope images of microbubbles observed after 1 min in the solutions from Figure 2b and 2c. These microbubbles are stabilized by *F*8*H*2Phos and dissolve completely after 10 minutes. In both cases (with and without NPs in the solution), the microbubbles have uncolored shells unlike the NP-stabilized microbubbles.

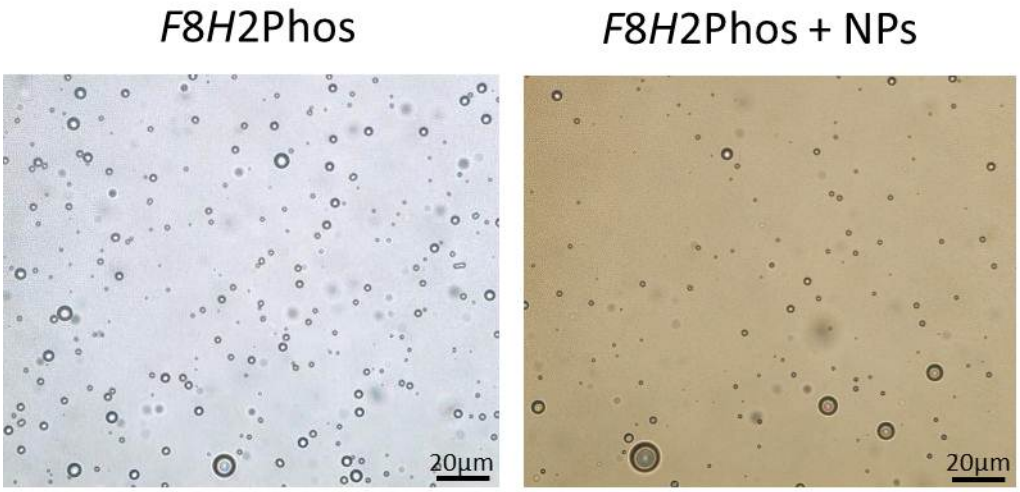

Figure SI-3 – Optical microscopy images of microbubbles stabilized for a few minutes in F8H2Phos solution with and without NPs. The solution composition corresponds to Figure 2b and 2c.

4) Temperature-mediated inflation and deflation of NP-stabilized microbubbles.

Figure SI-4 shows typical optical microscopy images of deflation of NP-stabilized microbubbles. The sample was first heated to 60°C in order to evoke the growth of microbubbles due to the water vapor pressure increase. The shell of the growing microbubble is fractured and remains a unique island on the bubble surface. During the cooling, the microbubble size decreases and the NP shell returns back to the percolated and rigid state.

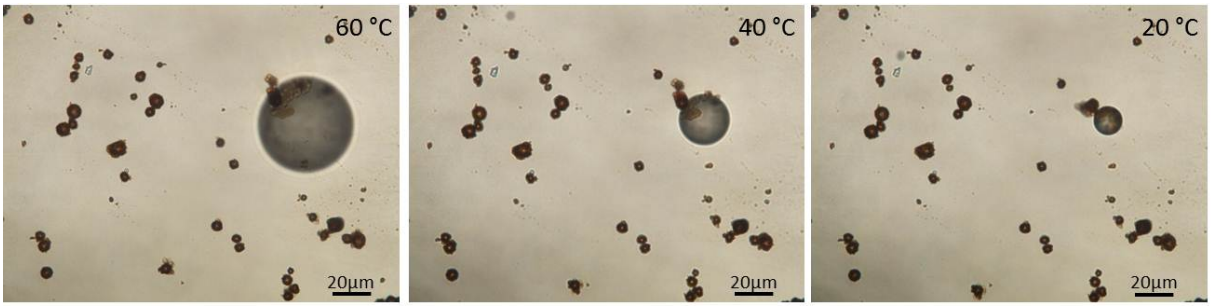

Figure SI-4 – Deflation of a NP-covered microbubble upon cooling.

5) Acoustical attenuation measurements of NP-stabilized microbubbles

NP-stabilized microbubbles shown in Figure 3d (after aging and big bubble disappearance) were injected in the acoustic cell for acoustic attenuation measurements. The attenuation coefficients are plotted versus frequency in Figure SI-5a for various times after the injection. Initially, the absorption maximum is located between 1 and 2 MHz. Because of flotation of the microbubbles, the attenuation decreases with time (Figure SI-5b) and disappears after 3000 s (about one hour). The curves have been fitted using a model for bubbles without shell described in[13]. The obtained size distribution maximum (Figure SI-5c) is initially located at 5 µm and is close to the maximum of the distribution from optical microscopy images (Figure 4). The biggest bubbles disappear faster than the smallest that is probably related to their fast flotation in the acoustic cell.

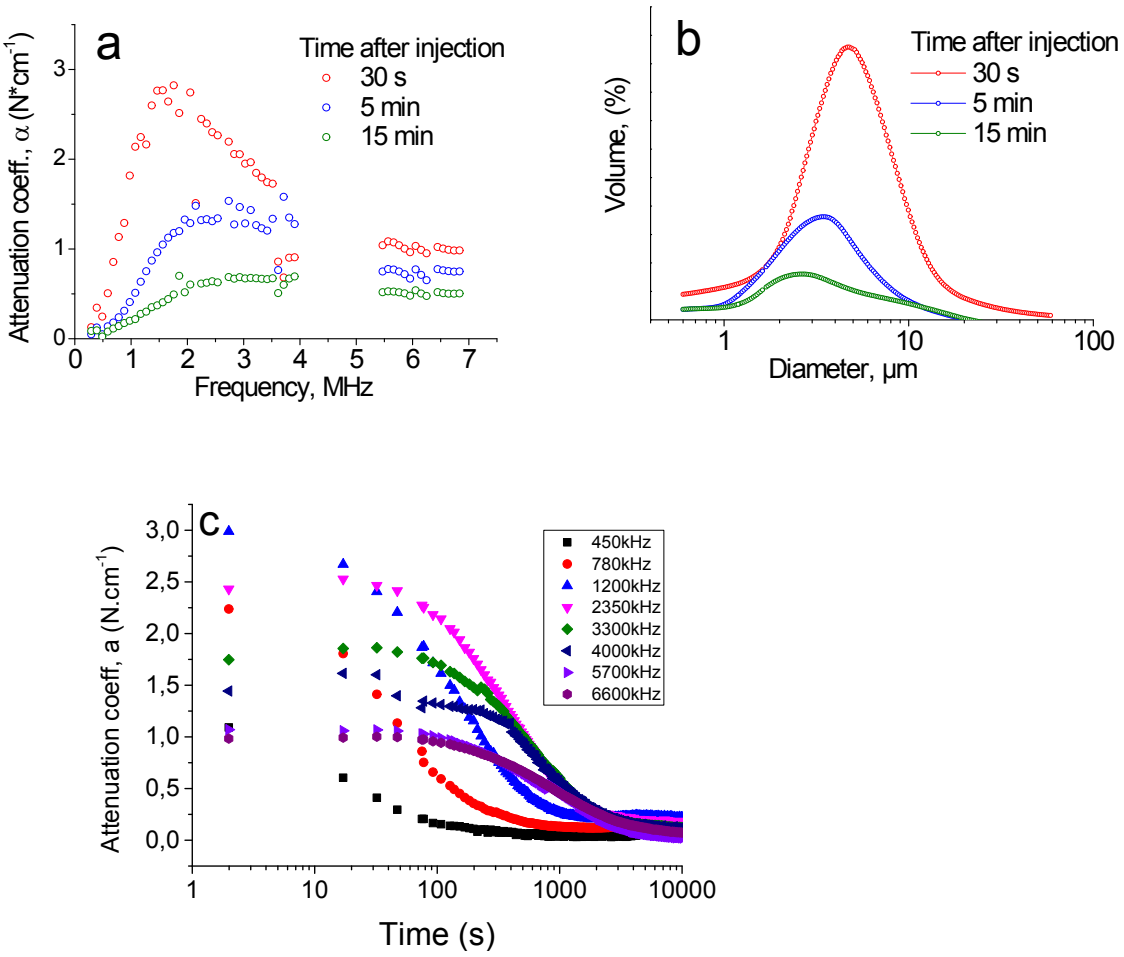

Figure SI-5 - Acoustical characterization of microbubbles stabilized by *F*8*H*2Phos and cobalt ferrite nanoparticles: a) variation of attenuation coefficient, α, as a function of ultrasound frequency at different time after injection in the acoustic cell; b) diameter distribution of bubbles calculated in the model of bubbles without shell; c) time evolution of attenuation coefficient at different frequencies. Characteristic frequencies for different bubble diameters: 13.3µm (450 kHz), 8µm (780 kHz), 5µm (1200 kHz), 2.5µm (2400 kHz), 1.8µm (3300 kHz), 1.04µm (5700 kHz), 0.9µm (6600 kHz).

6) TGA curves of NPs-*F*8*H*2Phos precipitate

Figure SI-6 shows the TGA curves of precipitate obtained by magnetic decantation of NP-surfactant mixtures at 0.1 M NaCl concentration (the condition of stabilization of microbubbles by the NPs). Pure nanoparticles exhibit the weight loss about 5% in the temperature range 50-450°C due to water and TMAH molecules adsorbed on the NP surface. When the *F*8*H*2Phos is added, the weight loss increases proving that the surfactant is adsorbed on the NPs. The concentration of free molecule (non-adsorbed) in the liquid is given by:

$$C_{F8H2Phos}{}^{supernat} = C_{F8H2Phos}{}^{total} - \frac{1000 * C_{NPs} * \psi_{F8H2Phos}}{(95.2 - \psi_{F8H2Phos}) * M_{F8H2Phos}}$$

$C_{F8H2Phos}{}^{total}$ is the concentration of surfactant in the liquid at the beginning, $C_{F8H2Phos}{}^{supernat}$ is the concentration of surfactant remaining in the supernatant (non-adsorbed molecules), C_{NPs} = 1 mg/mL is the concentration of nanoparticles, $\psi_{F8H2Phos}$ the weight percentage of surfactant in the precipitate (difference between the weight loss of pure NPs and NPs with surfactant), $M_{F8H2Phos}$ the molar weight of the surfactant (544 g/mol).

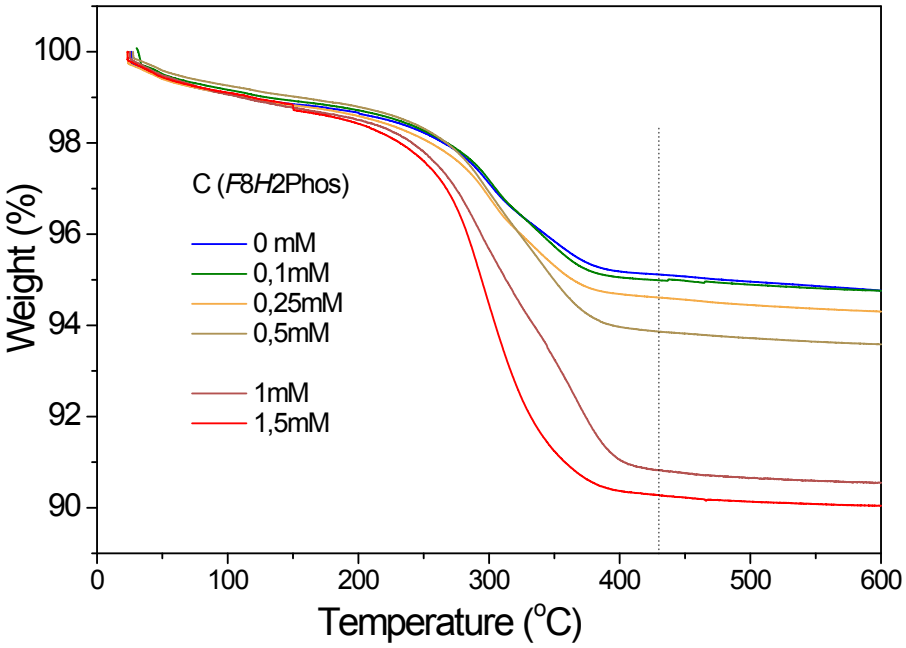

Figure SI-6 – Thermogravimetric analysis curves of magnetic precipitate recovered from NPs-*F*8*H*2Phos- solutions with various *F*8*H*2Phos concentrations.